Supporting Information

The Effect of the Dielectric Environment on Electron Transfer Reactions at the Interfaces of Molecular Sensitized Semiconductors in Electrolytes

Davide Moia,[1,2,*] Masato Abe,[1] Pawel Wagner,[3] Hiromu Saguchi,[1] Nagatoshi Koumura,[4] Jenny Nelson,[2] Piers R.F. Barnes,[2,*] Shogo Mori[1,*]

[1] Division of Chemistry and Materials, Faculty of Textile Science and Technology, Shinshu University, 3-15-1 Tokida, Ueda, Nagano 386-8567

[2] Department of Physics, Imperial College London, Prince Consort Road, SW7 2AZ, London

[3] ARC Centre of Excellence for Electromaterials Science, Intelligent Polymer Research Institute, University of Wollongong, Wollongong, NSW 2522, Australia.

[4] National Institute of Advanced Industrial Science and Technology, Interdisciplinary Research Center for Catalytic Chemistry, 1-1-1 Higashi, Tsukuba 305-8565, Japan.

*d.moia@fkf.mpg.de; piers.barnes@imperial.ac.uk; shogmori@shinshu-u.ac.jp

Section 1. Experimental method

Sample preparation: substrates (FTO glass or microscope glass slides) were cleaned before use, with the following procedure: 15 minutes ultrasonic cleaning in soap and DIW, 15 minutes ultrasonic cleaning in DIW, rinse with ethanol, air dry, UV ozone cleaning. The TiO_2 paste (DS 18 NR-T) was deposited on the substrates via doctor blading, resulting in films of about 4 µm thickness. The films were left on a hot plate at 120 °C for 10 minutes, before undergoing sintering in a furnace at 450 °C for 30 minutes (30 minutes heating ramp was used). A $TiCl_4$ treatment was performed for samples used in the dye regeneration study unless stated otherwise. A solution of 0.23 g $TiCl_4$ in water in 20 g of DIW was used, the samples were left in an oven at 70 °C for 30 minutes, before undergoing a second sintering step. Films used for the hole hopping studies were not exposed to a $TiCl_4$ treatment. The dyes were dissolved in toluene at a concentration of 0.3 mM. The samples were immersed in the dye solution after heating them up to a temperature of 80 °C and left in the solution for at least 18 hours to reach complete dyeing of the oxide surface, unless stated otherwise. Samples for hole hopping studies were fabricated on glass and sealed with an FTO slide and a polymer sealant. The sandwich structure was then infiltrated with the chosen electrolyte. Solar cell devices were fabricated on FTO, sealed with a second FTO slide covered with platinum which was sputtered on the substrate to obtain a semi-transparent layer of the material. Electrolytes containing a redox couple were infiltrated in these samples.

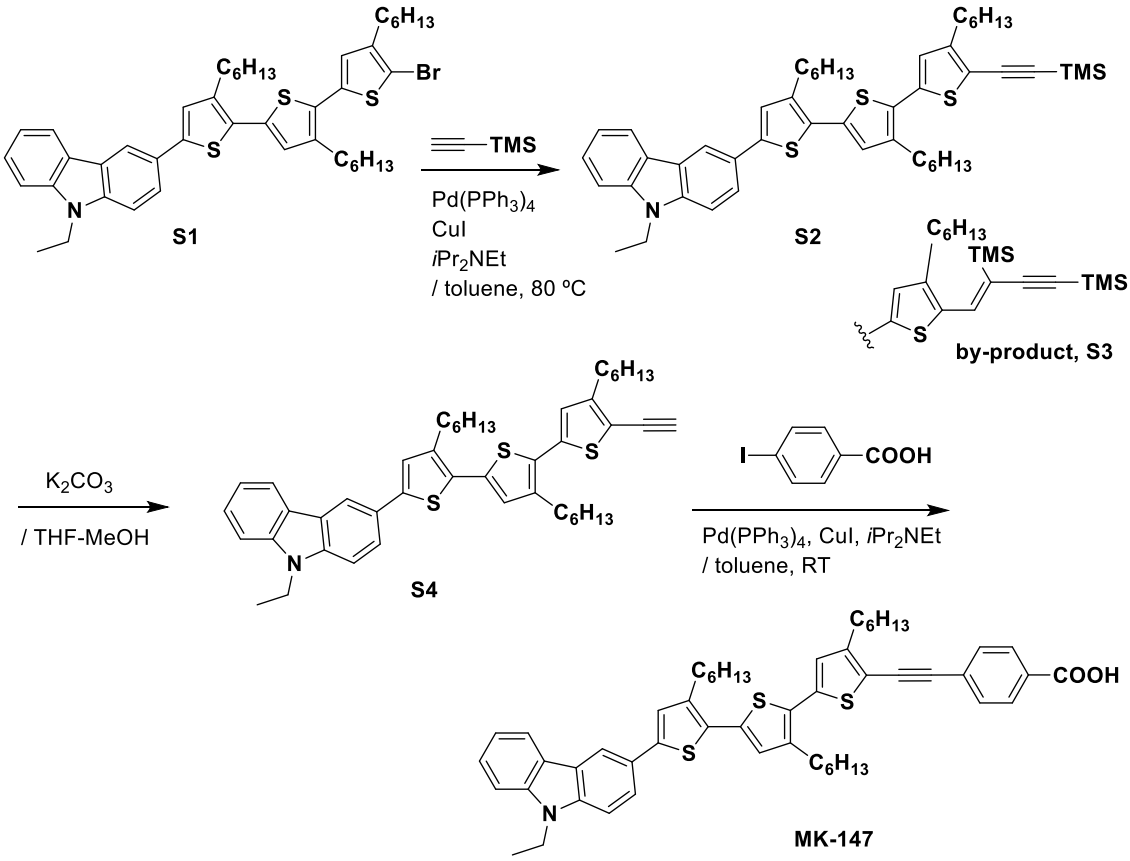
Section 2. Synthesis of MK147

General methods for synthesis

^{1}H NMR spectra were recorded on a Bruker Avance400 (400 MHz). ^{13}C NMR spectra were recorded on a Bruker Avance400 (100 MHz). Chemical shifts are denoted in δ-unit (ppm) relative to $CDCl_3$, THF-d_8. The splitting patterns are designated as follows: s (singlet); d (doublet); t (triplet); q (quartet); m (multiplet) and br (broad). Column chromatography was performed on silica gel (Kanto, Silica Gel 60N, spherical, 40-50 µm). Most of organic compound was finally purified by the preparative HPLC (YRU-880 detector from SHIMAMURA Tec.) through YMC-Pack CN column (250 x

20 mmI.D. S-10 μm, 12 nm, CN12S11-2520WT from YMC Co.Ltd). The solvents were distilled and dried, if necessary, by standard methods. Reagents and starting materials were used as obtained from Aldrich, Wako, Kanto Chemical, and TCI.

Synthesis of MK-147



9-Ethyl-3-(3,4',4''-trihexyl-5''-((trimethylsilyl)ethynyl)-[2,2':5',2''-terthiophen]-5-yl)-9H-carbazole, S2. 3-(5''-Bromo-3,4',4''-trihexyl-[2,2':5',2''-terthiophen]-5-yl)-9-ethyl-9H-carbazole, S1 was prepared by the method in the previous literature (*JACS* **2008**, *30*, 4202, Addition and Correction). A mixture of bromide **S1** (1.68 g, 2.17 mmol), trimethylsilylacetylene (0.42 ml, 3.04 mmol), copper iodide (67 mg, 0.760 mmol), tetrakis(triphenylphosphine)palladium (251 mg, 0.217 mmol), and 3 mL of diisopropylethylamine in dry toluene (10 mL) was heated to 80 °C for 12 h. After cooling, the reaction mixture was quenched with sat. NH_4Cl *aq*, and the water layer was extracted with EtOAc three times. The combined organic layer was washed with H_2O and brine, dried over $MgSO_4$, and evaporated under reduced pressure. The crude product was purified by column chromatography (hexane/EtOAc = 20/1) and successive HPLC (hexane/EtOAc = 20/1) to obtain a desired product **S2** (655 mg, 0.829 mmol, 38%) as a slightly yellow oil and a by-product **S3** (458 mg, 0.515 mmol, 24%). ^{1}H NMR of **S2** (400 MHz, $CDCl_3$) δ 8.31 (1H, br d, *J* = 1.8 Hz), 8.15 (1H, d, *J* = 7.8 Hz), 7.72 (1H, dd, *J* = 8.5, 1.8 Hz), 7.50 (1H, ddd, *J* = 8.2, 7.0, 1.1 Hz), 7.41 (1H, br d, *J* = 8.2 Hz), 7.40 (1H, d, *J* = 8.5 Hz), 7.26 (1H, ddd, *J* = 7.8, 7.0, 1.0 Hz), 7.20 (1H, s), 7.00 (1H, s), 6.90 (1H, s), 4.37 (2H, q, *J* = 7.2 Hz), 2.83 (2H, br t, *J* = 7.8 Hz), 2.78 (2H, br t, *J* = 7.8 Hz), 2.70 (2H, br t, *J* = 7.8 Hz), 1.79-1.63 (6H, m), 1.46 (3H, t, *J* = 7.2 Hz), 1.41-1.31 (18H, m), 0.95-0.89 (9H, m), 0.28 (9H, s), ^{13}C NMR of **S2** (100 MHz, $CDCl_3$) □ 149.2, 143.4, 140.7, 140.3, 139.5, 136.1, 134.8, 129.7, 128.6, 128.2, 126.2, 126.0, 125.2, 125.0, 123.8,

123.4, 122.9, 120.5, 119.1, 117.7, 117.5, 108.7, 108.6, 102.0, 97.5, 37.6, 31.71, 31.68, 31.58, 30.6, 30.4, 30.0, 29.7, 29.6, 29.5, 29.32, 29.26, 28.9, 22.64, 22.62, 22.60, 14.11, 14.09, 13.8, -0.02. ^{1}H NMR of by-product **S3** (400 MHz, $CDCl_3$) δ 8.33 (1H, br d, *J* = 1.8 Hz), 8.16 (1H, d, *J* = 7.8 Hz), 7.73 (1H, dd, *J* = 8.5, 1.8 Hz), 7.50 (1H, ddd, *J* = 8.2, 7.1, 1.1 Hz), 7.42 (1H, br d, *J* = 8.2 Hz), 7.40 (1H, d, *J* = 8.5 Hz), 7.28 (1H, ddd, *J* = 7.8, 7.1, 0.9 Hz), 7.21 (1H, s), 7.10 (1H, s), 7.06 (1H, s), 6.96 (1H, s), 4.37 (2H, q, *J* = 7.2 Hz), 2.86 (4H, br t, *J* = 7.8 Hz), 2.72 (2H, br t, *J* = 7.8 Hz), 1.81-1.61 (6H, m), 1.46 (3H, t, *J* = 7.2 Hz), 1.41-1.31 (18H, m), 0.96-0.90 (9H, m), 0.34 (9H, s), 0.28 (9H, s), ^{13}C NMR of by-product **S3** (100 MHz, $CDCl_3$) δ 144.6, 143.2, 140.5, 140.4, 139.8, 139.5, 136.1, 136.0, 135.9, 134.7, 130.7, 129.0, 128.2, 126.7, 126.0, 125.3, 125.1, 123.9, 123.4, 122.9, 120.6, 119.1, 118.7, 117.5, 110.7, 108.7, 108.6, 106.5, 37.6, 31.8, 31.6, 31.0, 30.6, 30.3, 29.7, 29.5, 29.3, 29.2, 29.0, 28.7, 22.65, 22.63, 22.60, 14.11, 14.08, 14.07, 13.8, 0.02, -1.88.

9-Ethyl-3-(5''-ethynyl-3,4',4''-trihexyl-[2,2':5',2''-terthiophen]-5-yl)-9*H*-carbazole, S4. To a solution of TMS-protected acetylene derivatives S2 (655 mg, 0.829 mmol) in THF-methanol (1:1, 10 mL) was added potassium carbonate (1.15 g, 8.29 mmol). The reaction mixture was stirred for 2 h at room temperature, and poured into water (100 mL). The mixture was extracted with EtOAc three times. The combined organic layer was washed with water and brine, dried over $MgSO_4$, and evaporated under reduced pressure. The crude product was purified by column chromatography (hexane/EtOAc = 50/1) and successive HPLC (hexane/EtOAc = 20/1) to obtain a desired product **S4** (453 mg, 0.631 mmol, 76%) as an yellow oil. ^{1}H NMR (400 MHz, $CDCl_3$) δ 8.32 (1H, br d, *J* = 1.7 Hz), 8.15 (1H, d, *J* = 7.8 Hz), 7.72 (1H, dd, *J* = 8.5, 1.7 Hz), 7.50 (1H, ddd, *J* = 8.2, 7.0, 1.1 Hz), 7.42 (1H, br d, *J* = 8.2 Hz), 7.39 (1H, d, *J* = 8.5 Hz), 7.27 (1H, br t, *J* = 7.2 Hz), 7.21 (1H, s), 7.01 (1H, s), 6.93 (1H, s), 4.37 (2H, q, *J* = 7.2 Hz), 3.55 (1H, s), 2.84 (2H, br t, *J* = 7.8 Hz), 2.79 (2H, br t, *J* = 7.8 Hz), 2.73 (2H, br t, *J* = 7.8 Hz), 1.80-1.64 (6H, m), 1.46 (3H, t, *J* = 7.2 Hz), 1.41-1.31 (18H, m), 0.98-0.90 (9H, m), ^{13}C NMR (100 MHz, $CDCl_3$) δ 149.4, 143.4, 140.6, 140.33, 140.28, 139.4, 136.5, 134.9, 129.4, 128.5, 128.0, 126.0, 125.9, 125.1, 124.9, 123.7, 123.3, 122.8, 120.4, 119.0, 117.3, 116.3, 108.6, 108.5, 84.2, 37.4, 31.7, 31.64, 31.58, 30.5, 30.4, 30.1, 29.7, 29.5, 29.3, 29.3, 29.2, 28.9, 22.64, 22.61, 22.58, 14.10, 14.07, 13.7.

4-((5''-(9-ethyl-9H-carbazol-3-yl)-3',3'',4-trihexyl-[2,2':5',2''-terthiophen]-5-yl)ethynyl)benzoic acid, **MK-147**. A mixture of acetylene derivatives **S4** (294 mg, 0.409 mmol), 4-iodobenzoic acid (112 mg, 0.450 mmol), copper iodide (8 mg, 0.041 mmol), tetrakis(triphenylphosphine)palladium (24 mg, 0.021 mmol), and 1 mL of diisopropylethylamine in dry toluene (3 mL) was heated to 80 ºC for 12 h. After cooling, the reaction mixture was quenched with sat. NH_4Cl *aq*, and the water layer was extracted with EtOAc three times. The combined organic layer was washed with H_2O and brine, dried over $MgSO_4$, and evaporated under reduced pressure. The crude product was purified by column chromatography (hexane/EtOAc = 2/1 → 1/1) to obtain **MK-147** (173 mg, 0.206 mmol, 50%) as yellow solids. ^{1}H NMR (400 MHz, $CDCl_3$) δ 8.32 (1H, br d, *J* = 1.7 Hz), 8.14 (1H, d, *J* = 7.7 Hz), 8.11 (2H, d, *J* = 8.5 Hz), 7.72 (1H, dd, *J* = 8.5, 1.7 Hz), 7.60 (2H, d, *J* = 8.5 Hz), 7.50 (1H, ddd, *J* = 8.1, 7.1, 1.0 Hz), 7.43-7.38 (2H, m), 7.27 (1H, ddd, *J* = 7.8, 7.1, 0.8 Hz), 7.20 (1H, s), 7.01 (1H, s), 6.98 (1H, s), 4.38 (2H, q, *J* = 7.2 Hz), 2.87- 2.77 (6H, m), 1.80-1.68 (6H, m), 1.46 (3H, t, *J* = 7.2 Hz), 1.41-1.32 (18H, m), 0.96-0.989 (9H, m), ^{13}C NMR (100 MHz, $CDCl_3$) δ 171.0, 149.4, 143.5, 140.8, 140.6, 140.4, 139.6, 137.4, 135.1, 131.1, 130.2, 129.6, 129.0, 128.6, 128.3, 128.2, 126.4, 126.0, 125.2, 125.1, 123.9, 123.4, 122.9, 120.6, 119.1, 117.5, 116.9, 108.74, 108.67, 95.8, 86.4, 37.7, 31.72, 31.69, 31.6, 30.6, 30.4, 30.2, 29.7, 29.6, 29.33, 29.29, 29.0, 22.7, 22.6, 14.13, 14.11, 13.8.

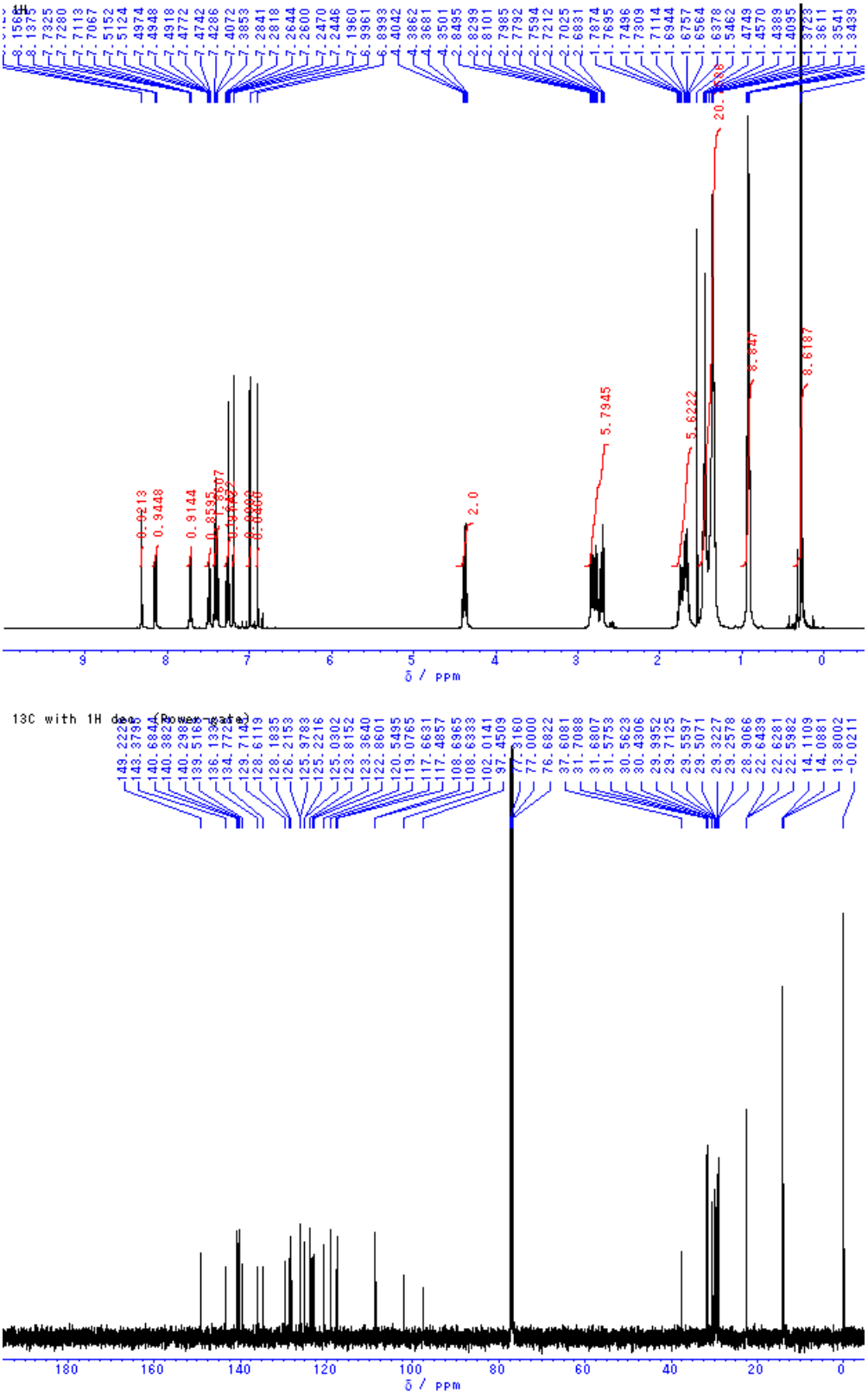


Figure S1. ^{1}H NMR and ^{13}C NMR of **S2**

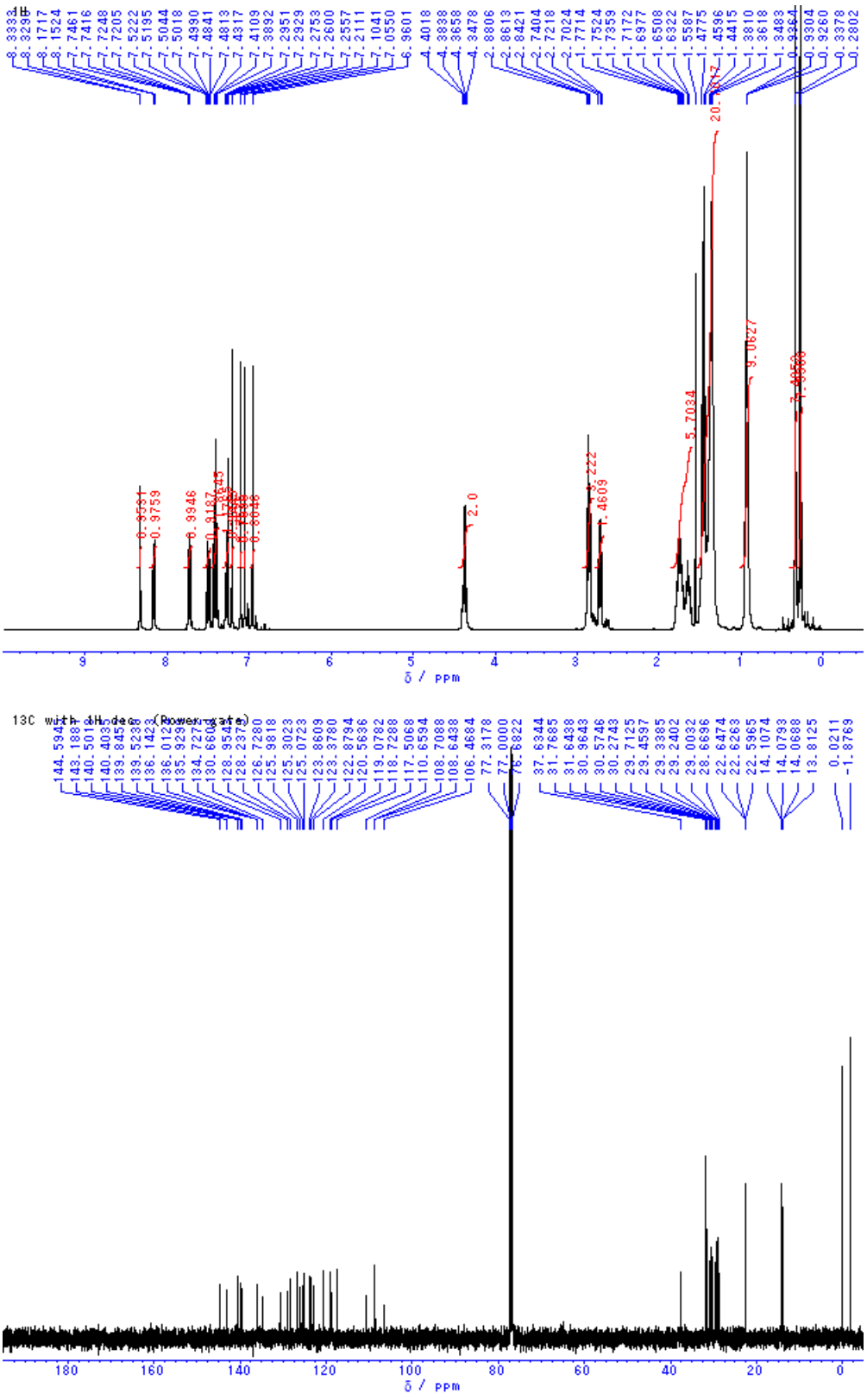


Figure S2. ^{1}H NMR and ^{13}C NMR of by-product **S3**

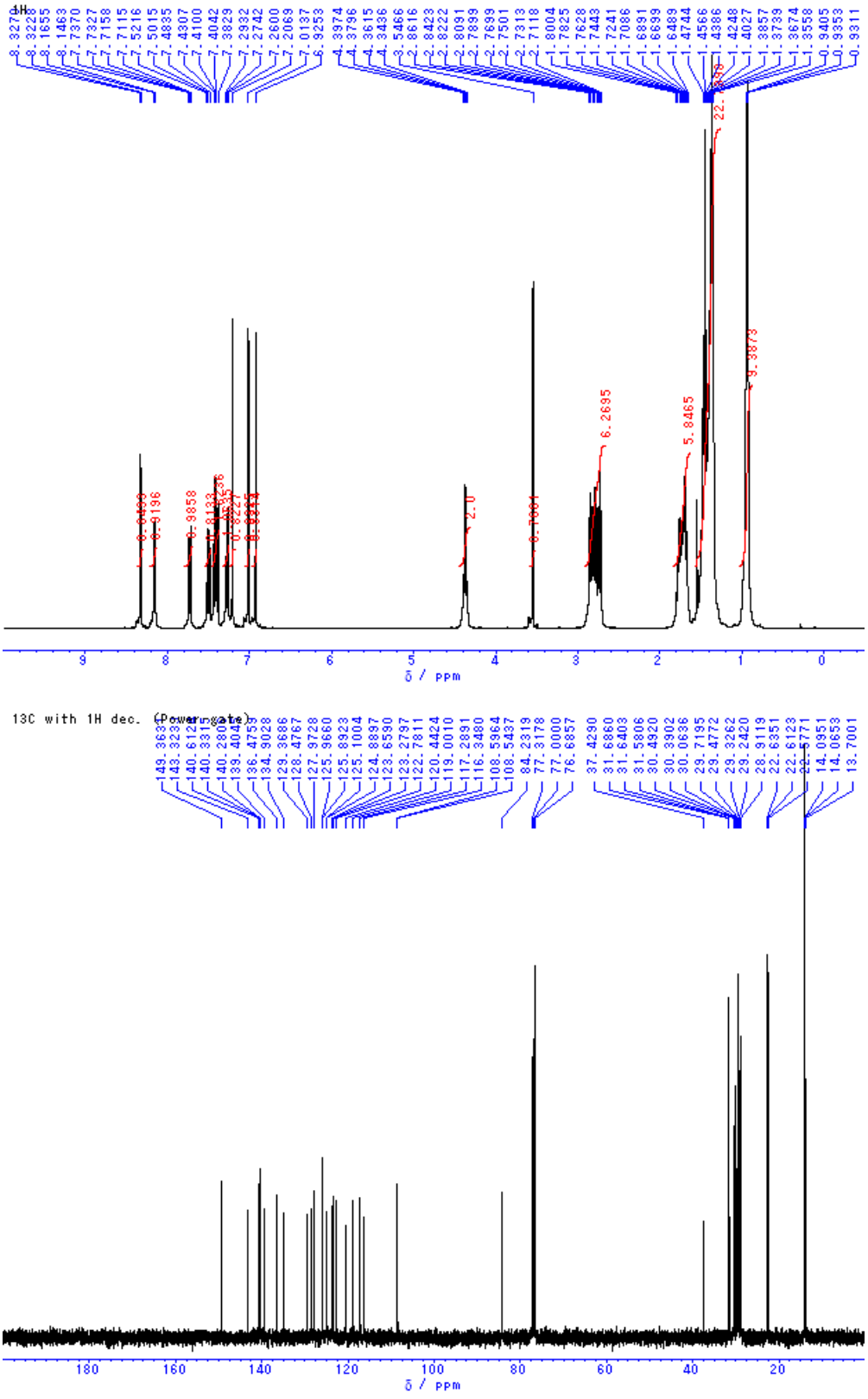


Figure S3. ^{1}H NMR and ^{13}C NMR of **S4**

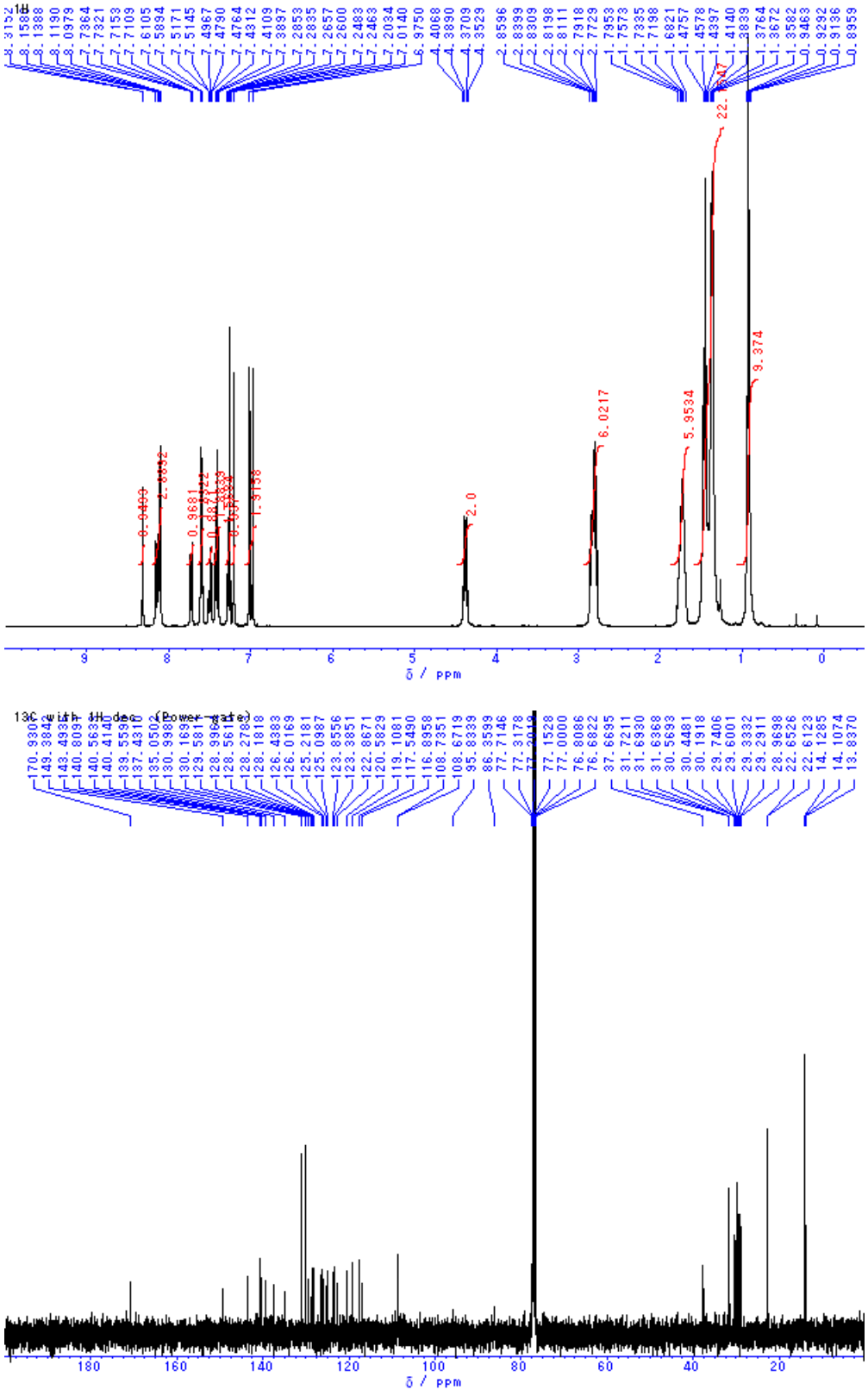


Figure S4. ^{1}H NMR and ^{13}C NMR of **MK-147**

Section 3. Notes on evaluation of activation energy from temperature dependent transient absorption anisotropy

The maximum value of r for which we are able to determine E_{act} is calculated as follows. We consider the early time scale value of r_{exp} for the measurement where, for each sample, this value is minimum (in most cases the highest temperature measurement, see anisotropy decays in Figure S9, S10, S11). We then subtract 3σ to this value, where σ is the noise level of the data after smoothing (see method in main text). This is to allow an accurate determination of t_r using Equation 4 in the main text.

Dielectric constants of solvents increase at lower temperature and a variation in the order of 50 to 100% is expected for the temperature range considered in this study.[2] By measuring temperature dependent rates of hole hopping for this study we have neglected this dependence.

Also, in a previous study we showed that molecular fluctuation might be responsible for the observed rate of hole hopping measured with electrochemical methods.[3] Indeed, such fluctuations are expected to introduce a thermal activation possibly related to viscosity of the solvent and which, however, ought to result in a constant value of the measured activation energy. This is not observed for most of the measurements reported here, suggesting that molecular fluctuations are unlikely to be the limiting factor to the rate of hole hopping.

Section 4. Monte Carlo simulation of transient absorption anisotropy

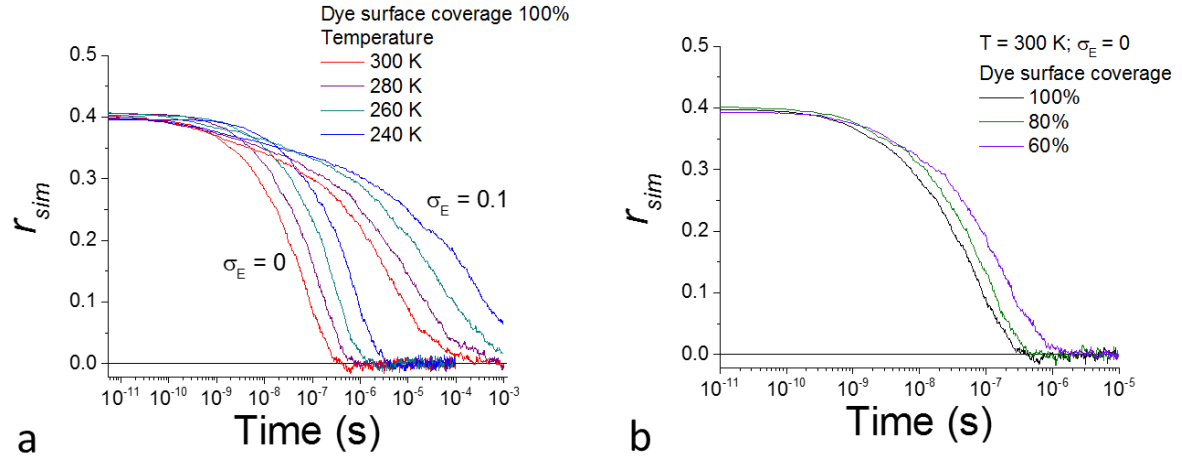


Figure S5. Monte Carlo simulations of transient absorption anisotropy for a dye sensitized cube. The hole transfer parameters for the simulations were J = 0.01 eV, λ = 1 eV. (a) Temperature dependent anisotropy profiles for the case with and without energetic disorder (σ_E is the standard deviation of the Gaussian distribution used to define the HOMO energies for the simulations). (b) Comparison of the anisotropy profiles for a disorder free system where different surface coverages are considered. For all simulation, the maximum value of anisotropy is set to 0.4, while for experiment this value is expected to be 0.3. As discussed in the supporting information of reference [1], for the case of randomly distributed orientation

of the dyes on the surface, the initial value of anisotropy set in the simulation does not affect the dynamics of the normalized anisotropy decay.

The transient anisotropy profiles were calculated from the simulation of holes diffusing on the surface of a cube of $(20\ nm)^3$ volume, randomly oriented in the three dimensions and with sites arranged in a square lattice with 1 nm lattice parameter. A transition dipole moment perpendicular to the surface of the cube was associated to the hole (oxidized dye), and the transient absorption anisotropy signal generated from the diffusion of the hole on the surface was calculated and averaged over 10^4 simulations. The hole transfer between neighboring sites (8 nearest neighbors) was calculated using Equation 1, where values of the reorganization energy and of the electronic coupling of 1 eV and 0.1 eV were chosen, consistently with our previous experimental estimates of these quantities for organic dyes adsorbed on TiO_2. For the case of simulations including energetic disorder, an energy extracted from a Gaussian distribution with standard deviation σ_E was associated to each site on the surface of the cube and used to calculate the ΔG_0 of the electron transfer reaction between each pair. The temperature dependent anisotropy profiles were then analysed similarly to the experimental data, as described in the experimental section.

Section 5. Protocol for temperature dependent transient absorption anisotropy measurements

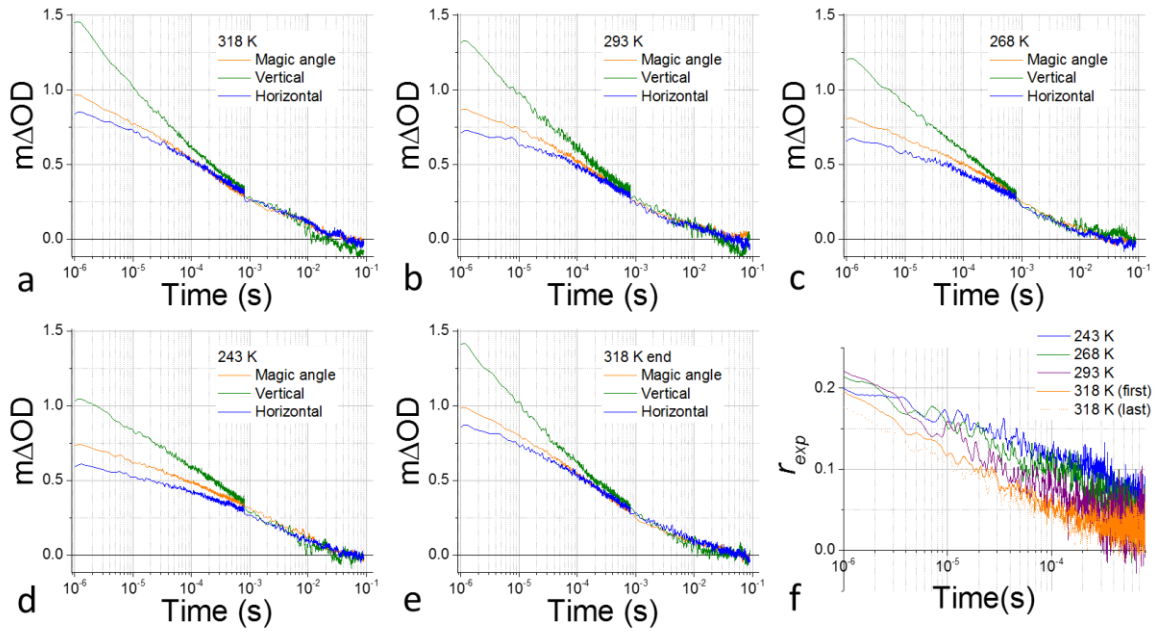


Figure S6. Measurement protocol for the temperature dependent transient anisotropy data shown in the main text. The sample (in this case MK2 on TiO_2 immersed in acetonitrile) was measured at (a) 318 K, (b) 293 K, (c) 268 K and (d) 243 K. Finally, a measurement at 318 K was repeated (e), to check the stability of the sample. (f) Anisotropy decays obtained before smoothing of the traces.

Section 6. Initial value of anisotropy for MK2 sensitized TiO_2 films

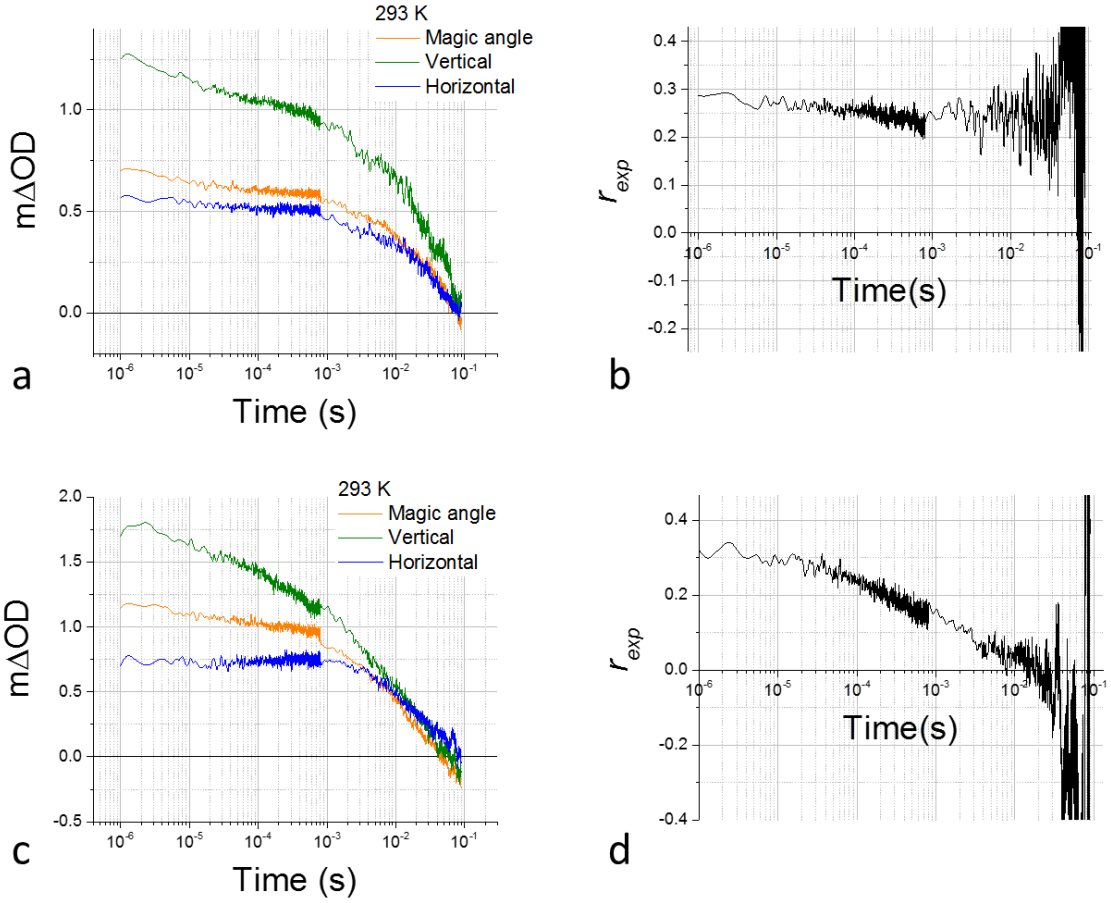


Figure S7. Measurement transient absorption and transient absorption anisotropy on low (< 50%) MK2 dye coverage obtained by sensitizing TiO_2 with a solution of 0.3 mM MK2 and 30 mM chenodeoxycholic acid (DCA) in a 1:1 mixture of acetonitrile and tert-butyl alcohol. (a) and (b) correspond to a sample immersed in acetonitrile, while (c) and (d) to a sample in dichloromethane. 10 Hz repetition rate was used for these measurements.

Figure S7 shows transient absorption anisotropy measurements on low dye loading MK2 sensitized TiO_2 samples. The value of anisotropy measured at the earliest timescale is approximately 0.3 for two different dielectric environments (acetonitrile and dichloromethane). This value is expected to be the highest value of the anisotropy for this experiment, corresponding to the absorption anisotropy probed at 780 nm, upon photoinduced electron injection. The fact that the value of 0.3 is observed for different experimental conditions suggests that the relative orientation of the ground state transition dipole moment excited through the polarized pump at 532 nm and the oxidized dye transition dipole moment associated to the probed absorption band at 780 nm does not significantly vary when the dielectric environment is changed. For this reason, we consider 0.3 as the starting value of anisotropy associated to the population of photogenerated holes.

Section 7. Temperature dependent anisotropy measurements

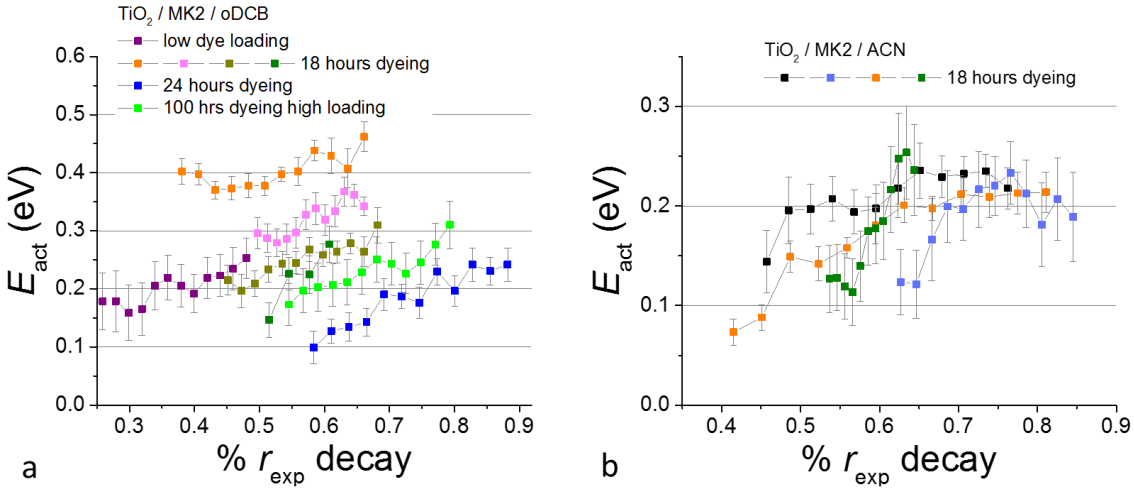


Figure S8. Reproducibility study for the estimation of activation energy of hole hopping in MK2 sensitized TiO_2 mesoporous films immersed in (a) oDCB and (b) acetonitrile, calculated from temperature dependent anisotropy measurements. The dataset of each graph correspond to different samples, nominally fabricated with the same method apart from the dyeing time (specified in the legend of the graphs).

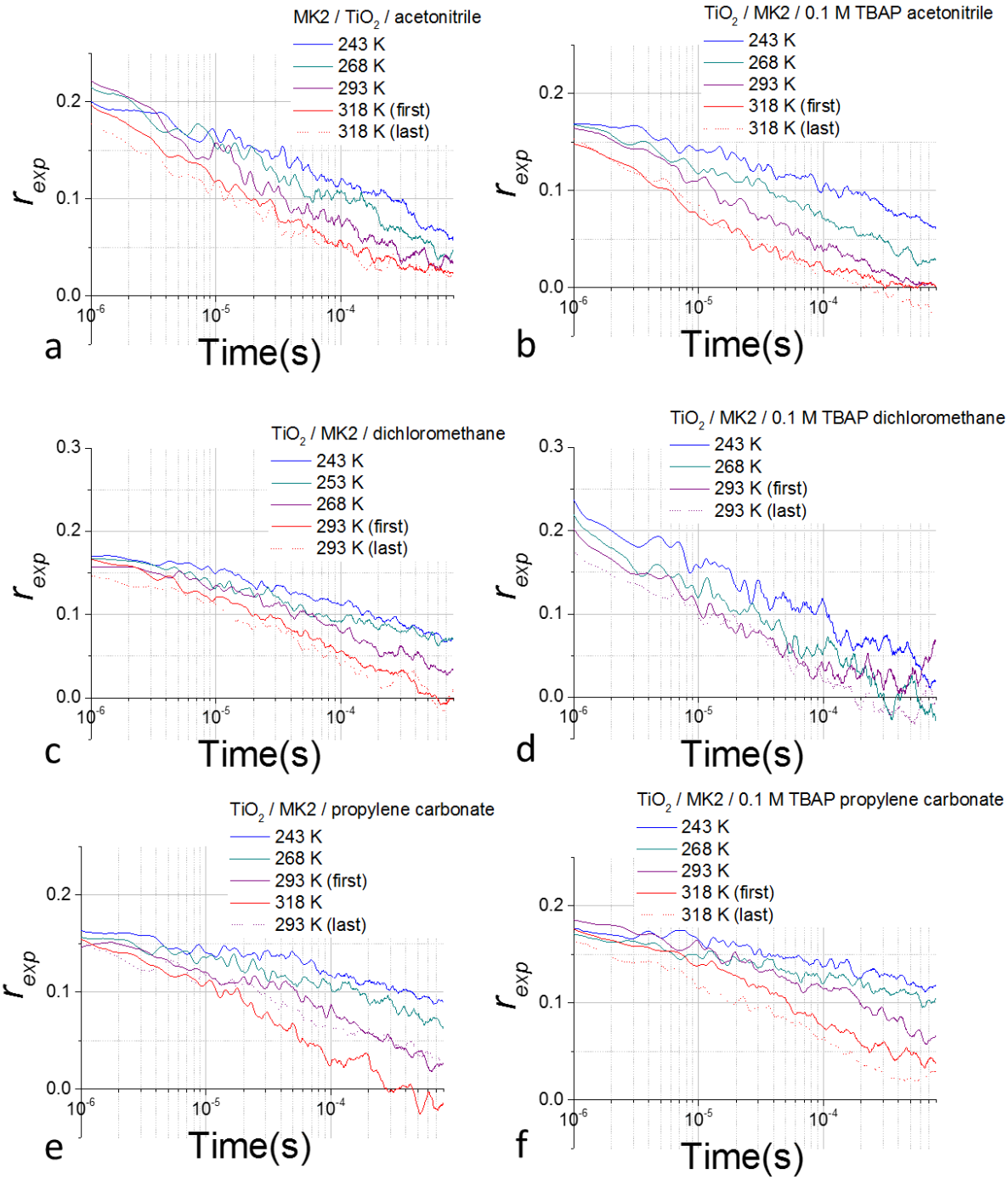
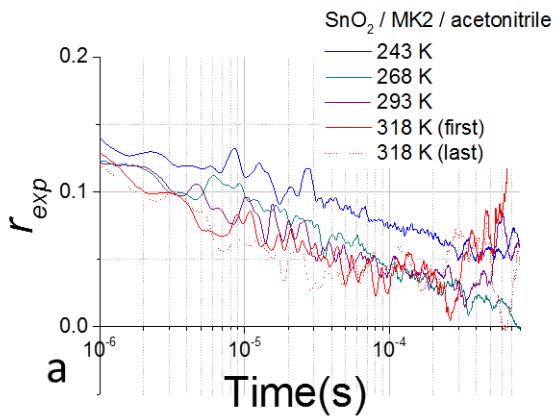
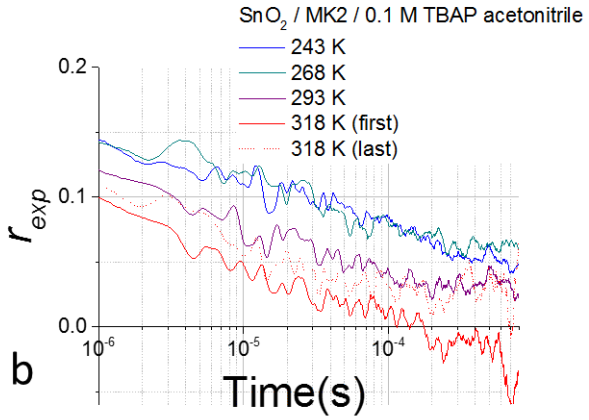
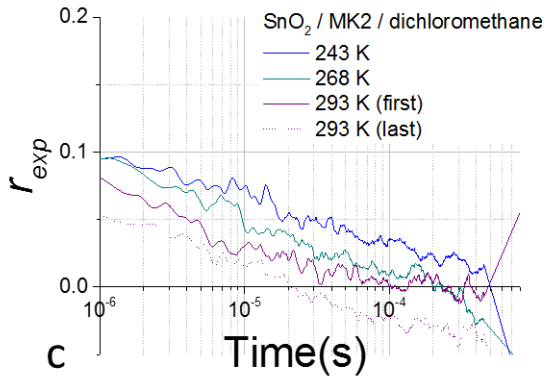
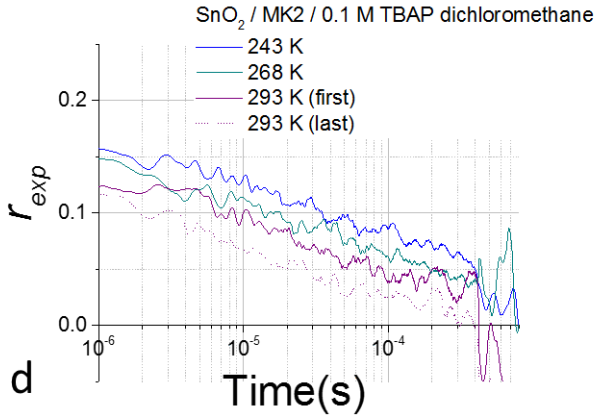


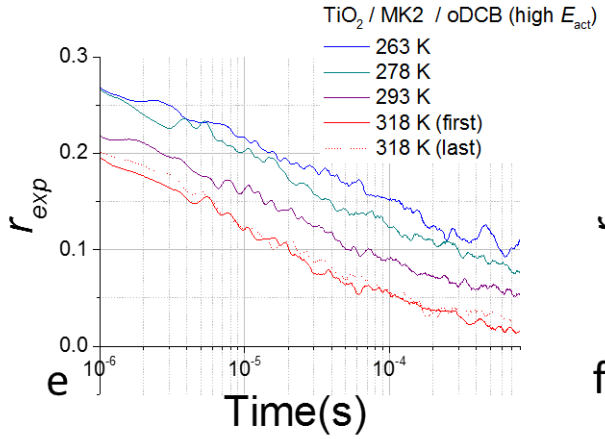
Figure S9. Measurements of temperature dependent transient absorption anisotropy on MK2 sensitized TiO_2 mesoporous films (left column) in different electrolytes and (right column) in 0.1 M TBAP dissolved in the same electrolytes as the left column.

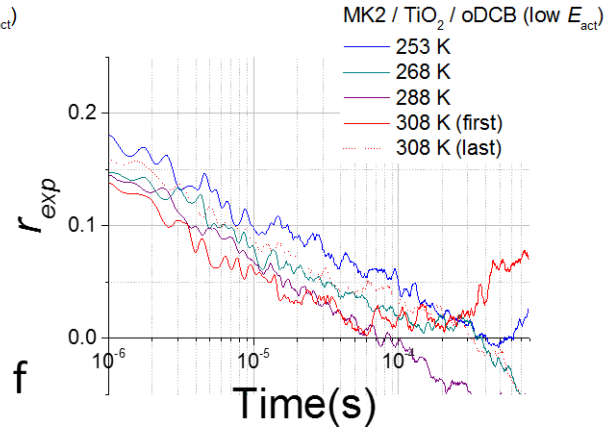

SnO2 / MK2 / acetonitrile
243 K
268 K
293 K
318 K (first)
318 K (last)
r exp
Time(s)
a


SnO2 / MK2 / 0.1 M TBAP acetonitrile
243 K
268 K
293 K
318 K (first)
318 K (last)
r exp
Time(s)
b


SnO2 / MK2 / dichloromethane
243 K
268 K
293 K (first)
293 K (last)
r exp
Time(s)
c


SnO2 / MK2 / 0.1 M TBAP dichloromethane
243 K
268 K
293 K (first)
293 K (last)
r exp
Time(s)
d


TiO2 / MK2 / oDCB (high Eact)
263 K
278 K
293 K
318 K (first)
318 K (last)
r exp
Time(s)
e


MK2 / TiO2 / oDCB (low Eact)
253 K
268 K
288 K
308 K (first)
308 K (last)
r exp
Time(s)
f

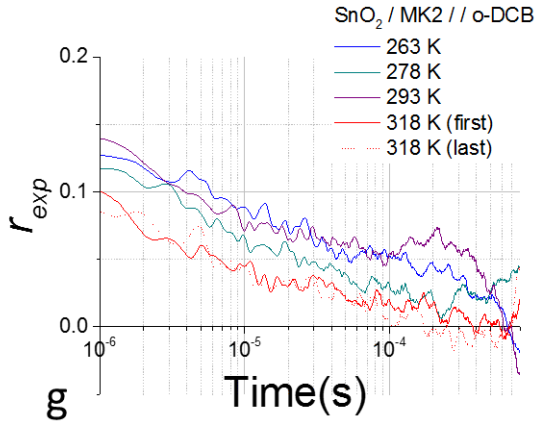

SnO2 / MK2 / / o-DCB
263 K
278 K
293 K
318 K (first)
318 K (last)
r exp
Time(s)
g

Figure S10. Measurements of temperature dependent transient absorption anisotropy on MK2 sensitized mesoporous films (TiO_2 or SnO_2) in different electrolytes, as indicated in the legend of each graph.

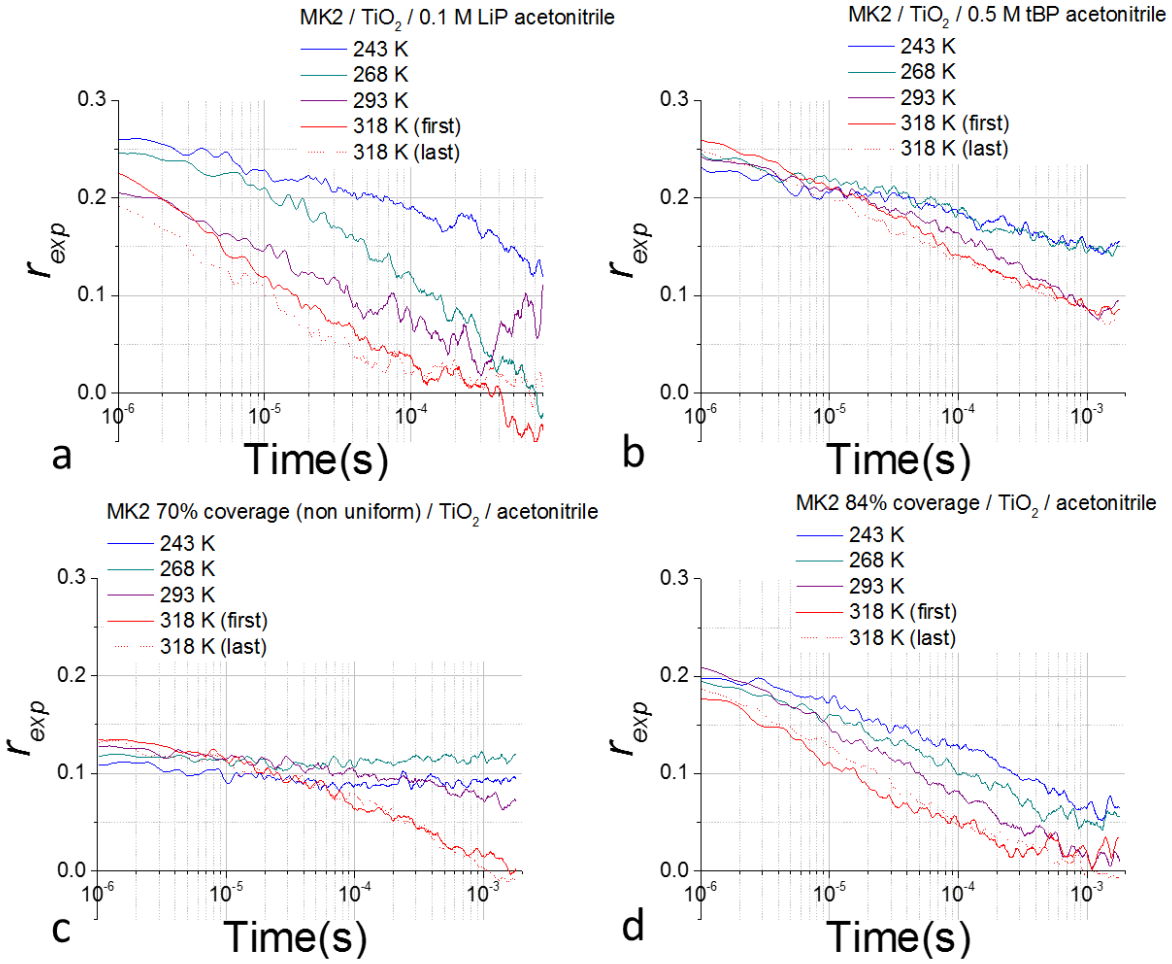


Figure S11. Measurements of temperature dependent transient absorption anisotropy on MK2 sensitized mesoporous TiO_2 films in acetonitrile. Effect of (a) lithium salts and (b) tert-butyl pyridine additive in the electrolyte, and (c)(d) effect of dye surface coverage. For both samples in (c) and (d) the sample was left in dichloromethane for 10 minutes, followed by rinsing with acetonitrile and sample assembly. The sample in (c) was sensitized for 7 hours instead of 18 hours, such that less uniform coverage is expected.

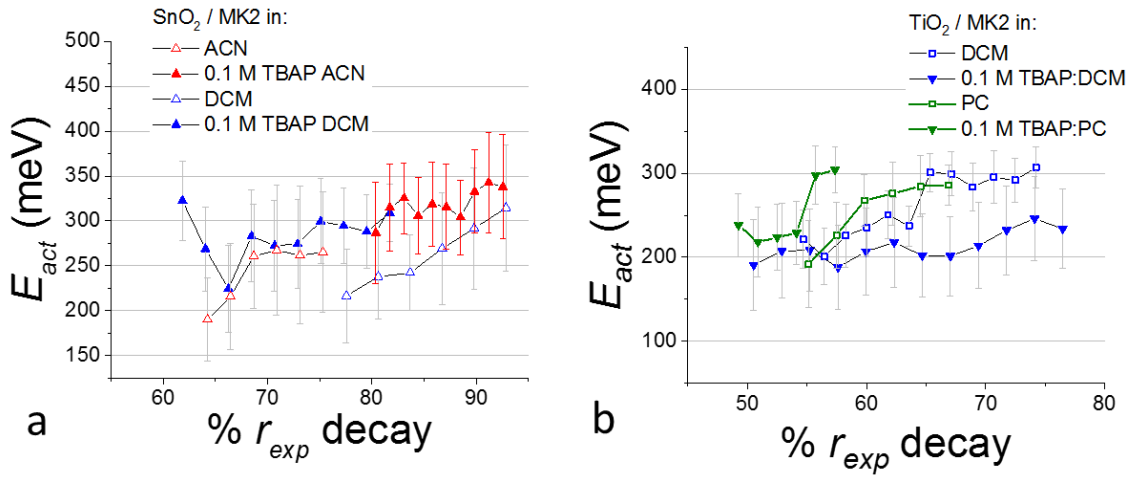


Figure S12. Measurements of activation energy for MK2 sensitized films showing the effect of TBAP salts, solvent and substrate. (a) MK2 on SnO_2, in acetonitrile or dichloromethane. (b) MK2 on TiO_2 in propylene carbonate (PC) and in DCM, with or without TBAP salts.

Section 8. Solvent dependent regeneration for the dyes MK3 and MK75

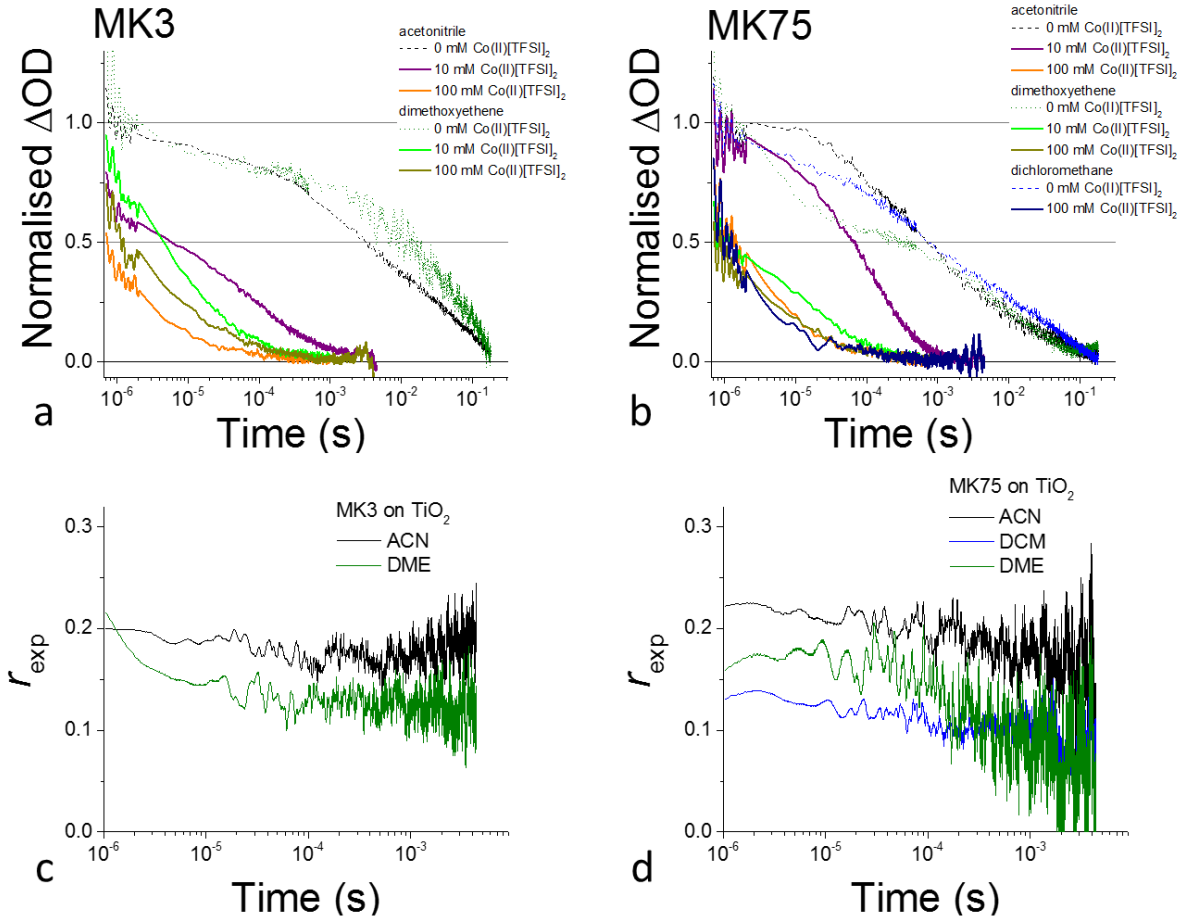


Figure S13. Transient absorption spectroscopy measurements on (a) MK3 and (b) MK75 sensitized solar cells using TiO_2 as mesoporous oxide and electrolytes containing a $Co^{(II/III)}(bpy)_3[TFSI^-]_{2/3}$

redox couple dissolved in different solvents. (c) and (d) show the transient absorption anisotropy decays for the dyes on TiO_2 immersed in pure solvents.

Section 9. Electron hole recombination

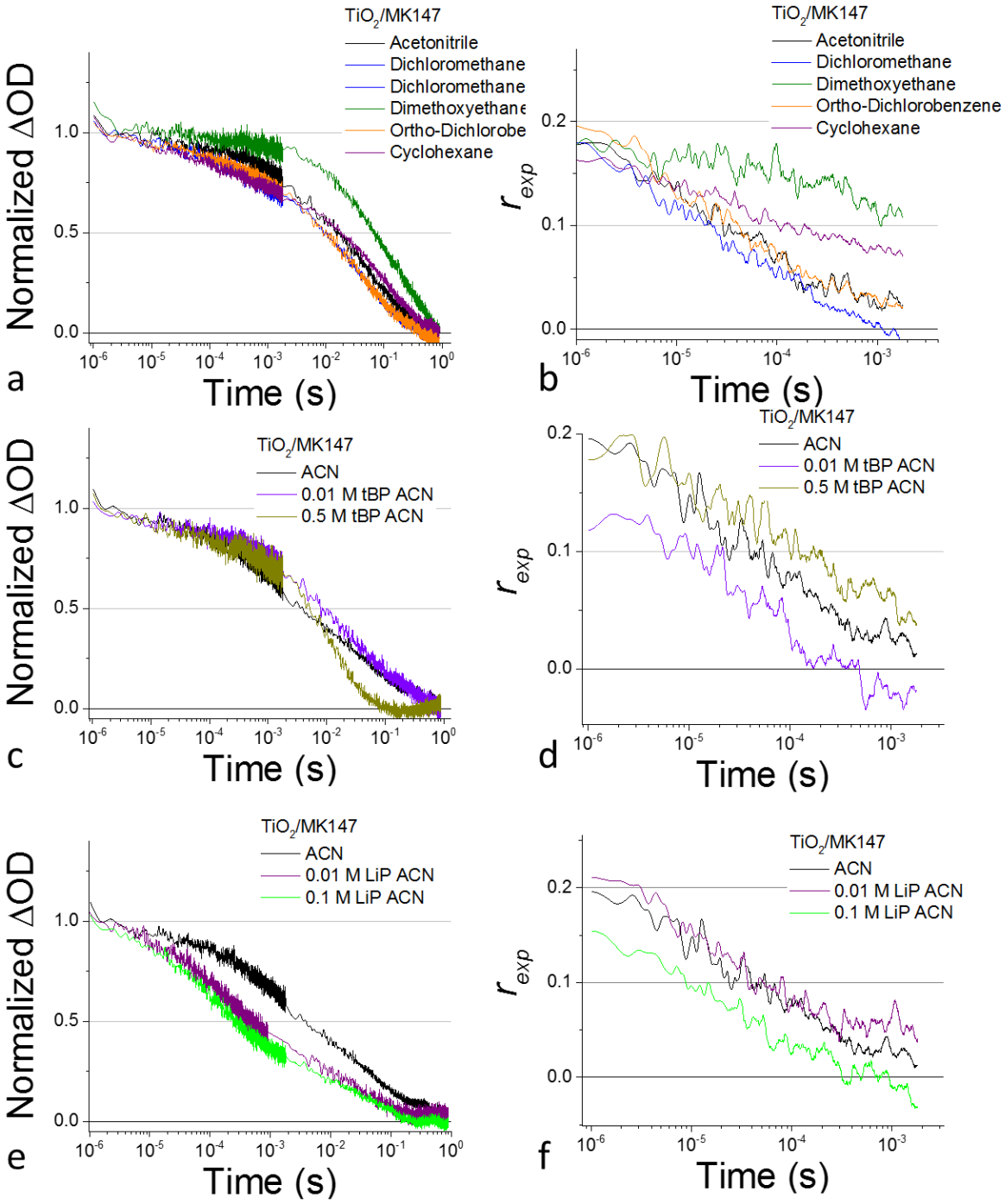


Figure S14. Transient absorption and transient absorption anisotropy measurements of MK147 sensitized TiO_2 mesoporous films in different inert solvents. Dependence of the kinetics of electron hole recombination and hole hopping on: (a, b) solvent; (c, d) addition of tert-butyl pyridine; (e, f) addition of lithium salt.

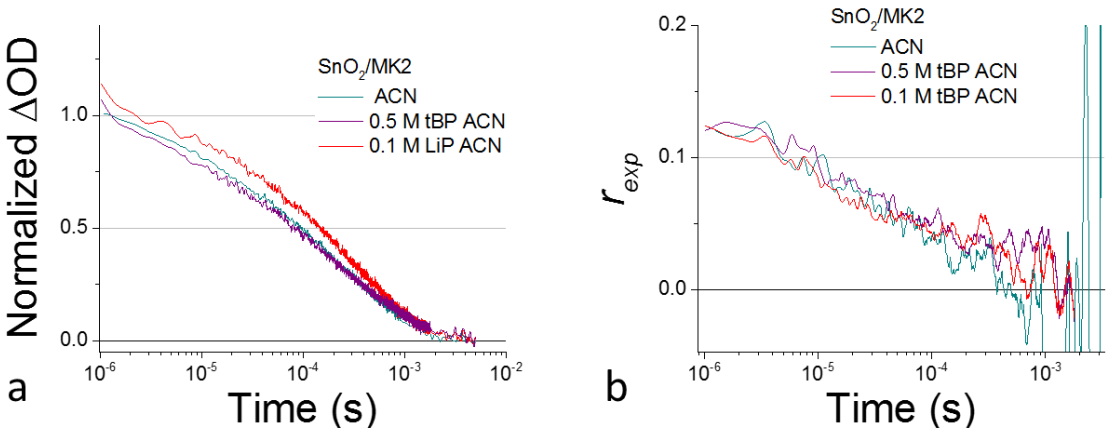


Figure S15. Transient absorption and transient absorption anisotropy measurements of MK2 sensitized SnO_2 mesoporous films in different inert solvents. Dependence of the kinetics of (a) electron hole recombination and (b) hole hopping on addition of tert-butyl pyridine and of lithium salt.

Section 10. Effect of redox couple and different inert cation and anion species on oxidized dye reduction kinetics

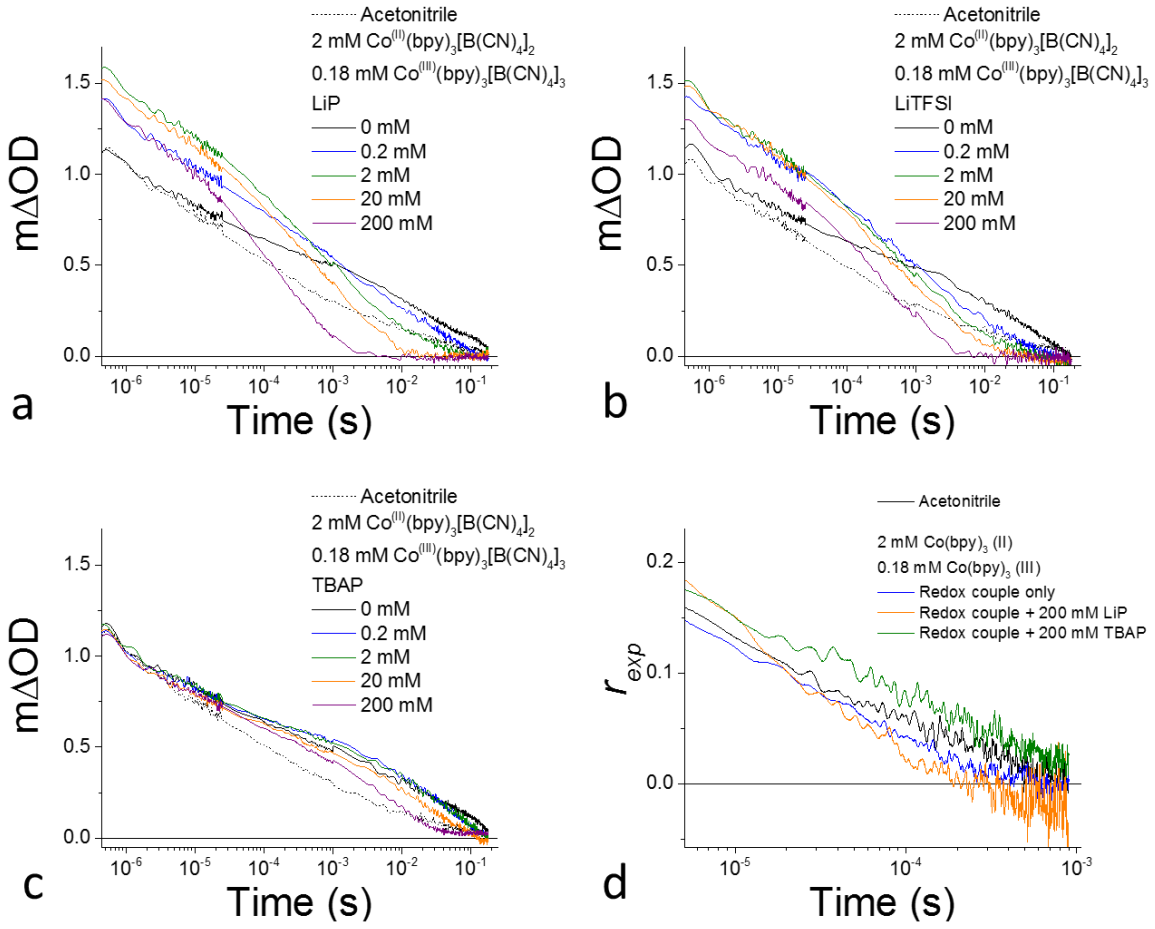


Figure S16. Effect of inert salts lithium perchlorate, lithium TFSI and tetrabutylammonium perchlorate to the kinetics of oxidized dye reduction in MK2 sensitized TiO_2 films in acetonitrile electrolytes, in the presence of a low concentration of cobalt redox couple.

Figure S16 illustrates the effect of different inert salts and of the cobalt redox-couple on the transient absorption and transient absorption anisotropy measurements of MK2 sensitized TiO_2 films. We observe a slow down in the kinetics of oxidized reduction when a low concentration of redox couple is added to the acetonitrile solvent. This result is counter intuitive, in that addition of the redox couple should contribute to faster oxidized dye reduction, while experiments show a clear slow down of such kinetics. The slow down effect was seen only for MK2 among four dyes, MK3, MK75, and MK147. Since the slow down effect was observed only with the low concentrations of Co complex, that are 10 and 2 mM for Figure S17 (see next section) and Figure S16, respectively, the effect is not due to direct interaction between the dyes and Co complex. Thus, one possibility is that the Co complex and counter anion stabilize the electron in the TiO_2 and the hole in a dye, and the effect is significant for the dye whose orbital is more delocalized. Note that MK2 has the widest absorption spectrum. Upon addition of lithium containing salts, the kinetics become faster, while it changes only slightly when considering TBAP salt. This result is consistent with the data presented in Figure 5 in the main text, where lithium ions in the electrolyte result in faster electron hole recombination reactions at all dye surface coverage conditions. The transient absorption anisotropy measurements in Figure S16d show that addition of lithium and TBA salts have slightly different

effects in this case compared to the case without redox-couple. In particular employing lithium salts results in a faster and less dispersive anisotropy profile while TBAP slows down slightly the anisotropy decay. These results show a similar trend with the dynamics of the hole population measurements (Figure S16a and c).

Section 11. Regeneration kinetics for MK2 and MK147 sensitized TiO_2 samples

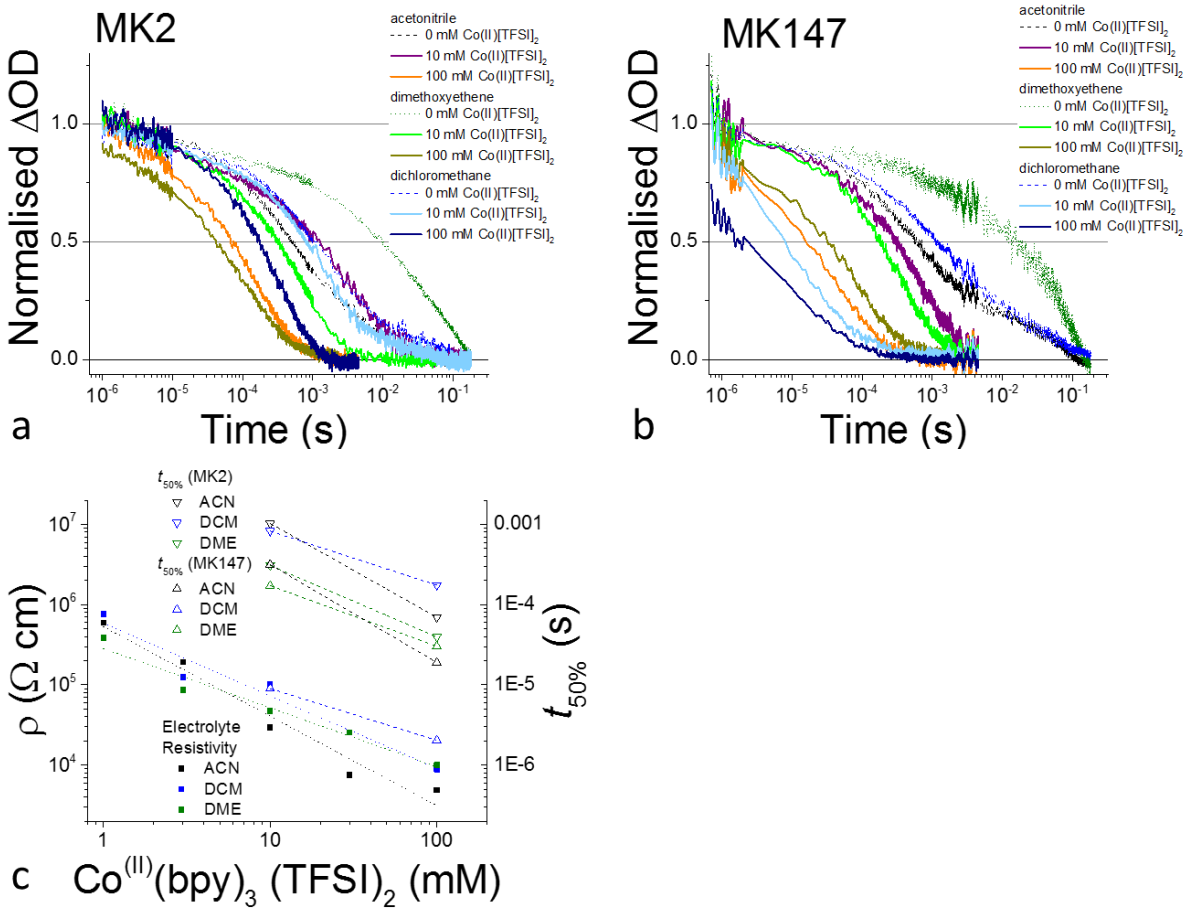


Figure S17. Transient absorption spectroscopy measurements on (a) MK2 and (b) MK147 sensitized solar cells using TiO_2 as mesoporous oxide and electrolytes containing either 10 mM or 100 mM of the Cobalt redox couple $Co^{(II)}(bpy)_3[TFSI^-]_{2/3}$ (with 0.9 mM and 9 mM of $Co^{(III)}(bpy)_3[TFSI^-]_{2/3}$ respectively) dissolved in different solvents. (c) Comparison between the trend in regeneration half life and in electrolyte resistivity against electrolyte concentration. The resistivity was measured using impedance spectroscopy applied to samples where a volume of electrolyte with known area and thickness was sandwiched between two platinum electrodes. The dotted lines are linear fits in log-log scale to the data and their discussion is presented in the main text.

Section 12. Recombination and regeneration kinetics for MK2:DCA sensitized TiO_2 samples

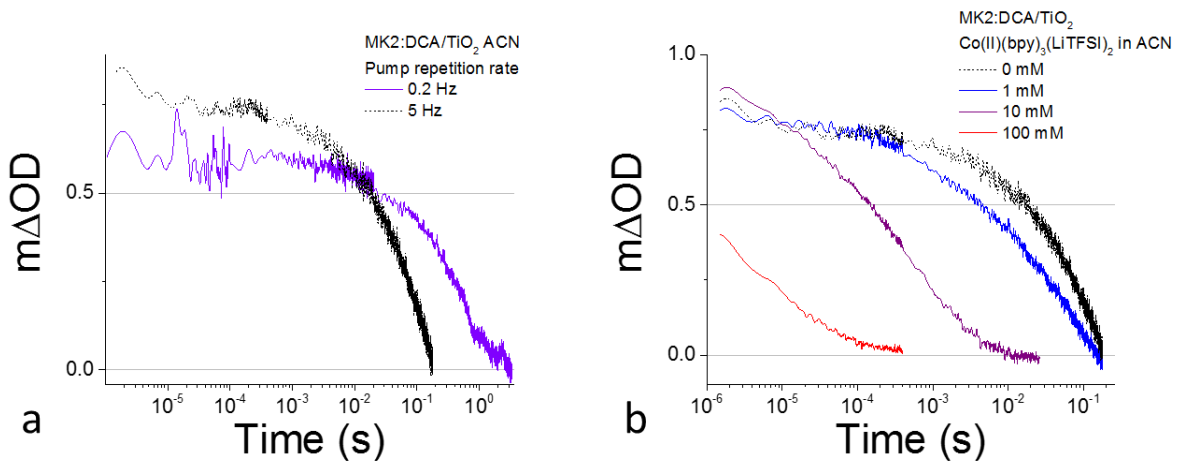


Figure S18. Transient absorption spectroscopy on MK2:DCA sensitized TiO_2 films. The sample in (a) was immersed in acetonitrile and the signal decay is associated to recombination of holes with electrons in the TiO_2. For the data in (b) different concentrations of the cobalt redox couple were added to the acetonitrile electrolyte for the solid lines, which we associate to regeneration of the photo-oxidized dye by the cobalt redox couple.

Section 13. Effect of lithium ions on kinetics of regeneration

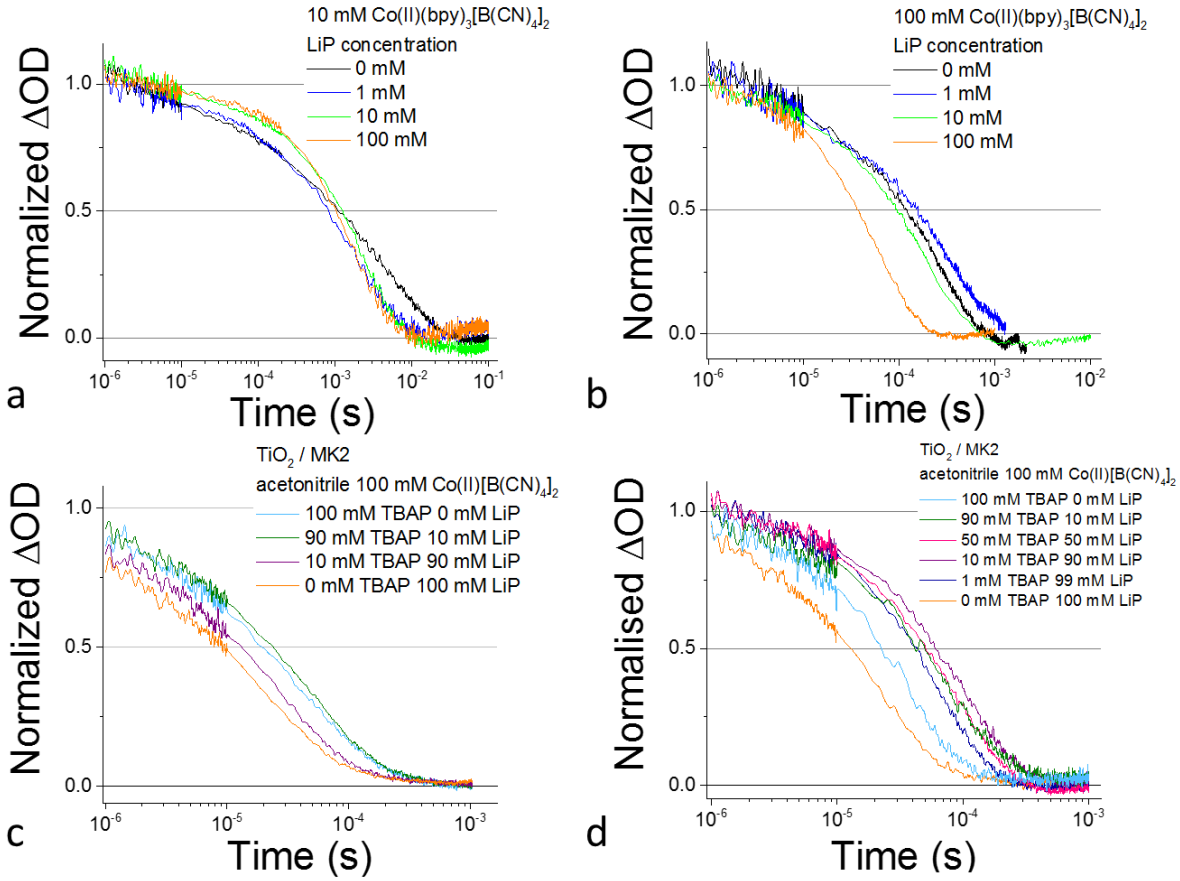


Figure S19. (a) and (b) show comparisons of the kinetics of regenerations in MK2 sensitized solar cells with different concentrations of LiP salt in acetonitrile electrolytes with 10 mM and 100 mM concentration of $Co^{(II)}(bpy)_3[B(CN)_4^-]_2$. (c) Effect of LiP and TBAP in solar cells with the same total concentration of inert supporting electrolyte ([TBAP]+[LiP] = constant). (d) is a repeat of (c) where the 100 mM TBAP sample was fabricated the day after compared to the others from a film of the same batch.

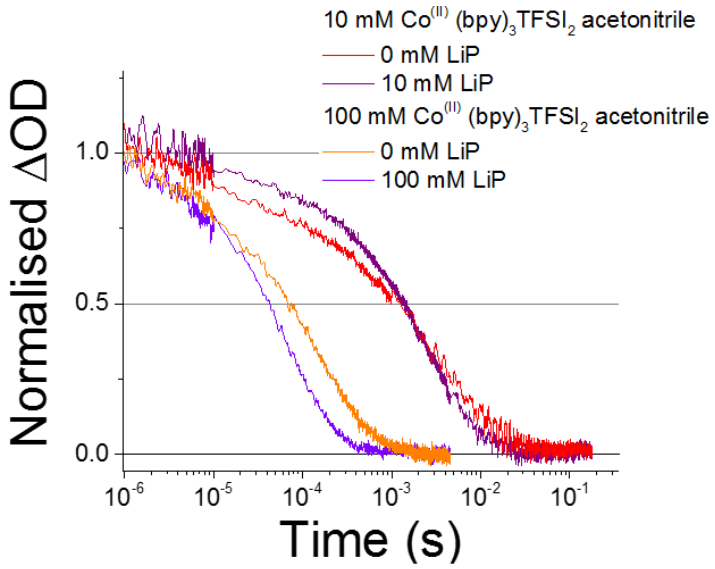


Figure S20. Comparisons of the kinetics of regenerations in MK2 sensitized solar cells with different concentrations of LiP salt in acetonitrile electrolytes with 10 mM and 100 mM concentration of $Co^{(II)}(bpy)_3[TFSI^-]_2$.

Section 14. Solubility of MK2 and MK147 in different solvents

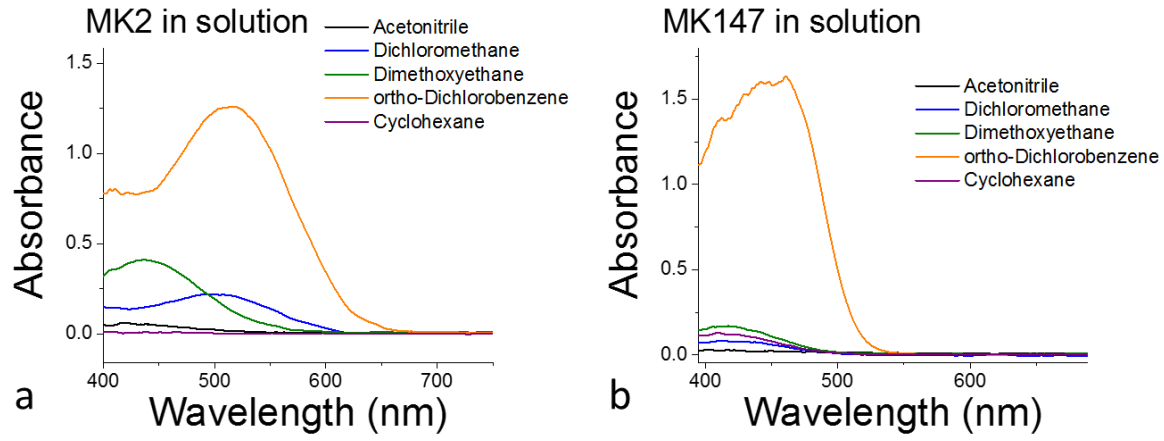


Figure S21. Absorption spectrum of MK2 and MK147 dye dissolved in solutions using the solvents considered in this study. The magnitude of the absorbance spectra indicates the solubility of the dyes in each solvent.

Supporting references

(1) Moia, D.; Szumska, A.; Vaissier, V.; Planells, M.; Robertson, N.; O'Regan, B. C.; Nelson, J.; Barnes, P. R. F. Interdye Hole Transport Accelerates Recombination in Dye Sensitized Mesoporous Films. *J. Am. Chem. Soc.* **2016**, *138* (40), 13197–13206. https://doi.org/10.1021/jacs.6b04956.

(2) Wang, P.; Anderko, A. Computation of Dielectric Constants of Solvent Mixtures and Electrolyte Solutions. *Fluid Phase Equilib.* **2001**, *186* (1–2), 103–122. https://doi.org/10.1016/S0378-3812(01)00507-6.

(3) Mosconi, E.; Moia, D.; Pastore, M.; Frost, J. M.; Angelis, F. De; Barnes, P. R. F.; Nelson, J. Effect

of Molecular Fluctuations on Hole Di Ff Usion within Dye Monolayers. **2014**. https://doi.org/10.1021/cm502629c.